2024. Journal of Arachnology 52:1–8

An assessment of the mechanosensory responses of peg sensilla on scorpion pectines

Hannah M. Peeples and Douglas D. Gaffin: Department of Biology, University of Oklahoma, Norman, OK 73019 USA; E-mail: ddgaffin@ou.edu

Abstract. Scorpions possess midventral touch/taste organs called pectines, which may be important for learning the nuances of the substrate during navigation as well as the detection of pheromones, spermatophores, and food. The pectines possess thousands of minute structures called peg sensilla that are responsive to both chemicals and mechanical deflection of the peg shaft. While much is known about the chemical responsiveness of the pegs, very little is known about their mechanosensory properties. Here we ask if the peg mechanosensory response is "all-or-nothing" or graded depending on the intensity of stimulation. We made electrophysiological recordings of neural activity from individual peg sensilla while deflecting the peg to elicit apparent mechanosensory responses. Our records show the presence of a rapid firing (>100 Hz), quickly adapting waveform that is indicative of a mechanoreceptor and appears to be independent of previously identified chemo-responsive cells. We tested mechanosensory response dynamics in two ways. The first test focused on a shorter-duration touch versus a longer-duration touch, while the second focused on a smaller deflection versus a larger deflection. Both pairs of stimulations (short vs long touch; small vs large touch) produced repeatable and statistically distinct responses in terms of spiking frequency. These results indicate the mechanosensory responses of peg sensilla are graded, which sheds light on the textural resolvability of the pectines and informs models of the type of information that scorpions obtain while assessing surfaces in their environment.

Keywords: Electrophysiology, mechanoreceptor, sensilla, resolvability
https://doi.org/10.1636/JoA-S-22-052

Scorpions possess ornate mid-ventral touch/taste organs called pectines, which may be important for learning the nuances of the substrate during navigation (Gaffin & Brayfield 2017; Musaelian & Gaffin 2020; Prévost & Stemme 2020; Gaffin et al. 2022) as well as recognizing pheromones (Gaffin & Brownell 1992; Melville et al. 2003; Taylor et al. 2012) and spermatophores (Polis & Farley 1979) for reproduction. The morphology of these sensory organs and their chemosensory and mechanosensory abilities appear to support the detection of textures and chemical cues that allow scorpions to find food, navigate, avoid predators, and reproduce (Krapf 1986; Brownell 2001; Gaffin & Brownell 2001; Gaffin & Curry 2020; Ortega-Escobar et al. 2023).

Scorpion pectines extend from the mid-ventral mesosoma and include teeth that possess tens to hundreds of minute structures called peg sensilla (Foelix & Müller-Vorholt 1983) that are responsive to both chemicals and mechanical deflection of the peg shaft (Gaffin & Brownell 1997; Knowlton & Gaffin 2009, 2010, 2011a). Each peg sensillum is anchored in a flexible cuticular socket. For *Paruroctonus utahensis* (Williams, 1968), the scorpions used in this study, the sensilla are spaced about 7 μm apart. A narrow slit at the tip of the shaft opens to a fluid-filled lumen containing the unbranched dendritic outer segments of several (at least 10) apparent chemosensory neurons (Ivanov & Balashov 1979; Foelix & Müller-Vorholt 1983; Wolf 2017). Morphological studies also show that an additional neuron ends near the peg base and contains many tubular bodies, which is characteristic of mechanoreceptors (Foelix & Müller-Vorholt 1983). Furthermore, the information processed by the pectines appears to maintain topographic order in the central nervous system, at least for the chemosensory neural projections (Brownell 1998, 2001; Wolf 2008; Wolf & Harzsch 2012; Hughes & Gaffin 2019; Drozd et al. 2020). There also appears to be reflexive control of the position of the pectinal teeth relative to the substrate as triggered by the mechanosensory hair sensilla on the pecten spine (Drozd et al. 2022).

While much is known about the chemical responsiveness of peg sensilla (Gaffin & Brownell 1997; Knowlton & Gaffin 2011b), studies on the mechanoreceptor capabilities of the peg sensilla are limited (Gaffin & Brownell 1997; Gaffin 2001). The mechanoreceptor recordings reported thus far appear to indicate a larger spike waveform as compared to chemosensory action potentials (Gaffin 2001), but the response dynamics have yet to be tested. A better understanding of the mechanosensory responses of peg sensilla is needed to shed light on the pattern detection potential of the peg matrices, which can help inform models of scorpion navigation, along with food, shelter, and/or spermatophore recognition (Krapf 1986; Brownell 2001; Gaffin & Brownell 2001).

We made multiple extracellular electrophysiological recordings from peg sensilla while physically deflecting the pegs to elicit mechanoreceptor responses. We assessed the shapes of the spike waveforms and the patterns of mechanically induced neural activity. We also tested the difference between shorter- and longer-duration stimulations and between smaller and larger deflections. Our results show that the mechanosensory response is of high frequency and that it quickly adapts and recovers. Further our results suggest the response is graded, which has implications for the information capacity of the peg matrices for texture discrimination.

METHODS

Collection and care of scorpions.—Female adult desert sand scorpions (*Paruroctonus utahensis*) were collected from sand dunes near Monahans, Texas using ultraviolet flashlights. The scorpions were housed in the laboratory in large glass jars (3.8 l) containing 100 ml sand and a half piece of PVC pipe for shelter. The holding room was on a 14:10h (L:D) cycle in which the lights came on at 06:00 and turned off at 20:00. The holding room temperature was ~25°C and the relative humidity ~48%. Each animal was given one small cricket every other week and three sprays of water every week. After each experiment, the scorpion was returned to its jar and not reused for additional electrophysiology.

A total of 14 female scorpions were used in this study for a total of 7.29 hours of recording time. We used only female scorpions for two reasons: (1) to reduce variation related to intersex differences and (2) because female sand scorpions are more faithful to their burrows

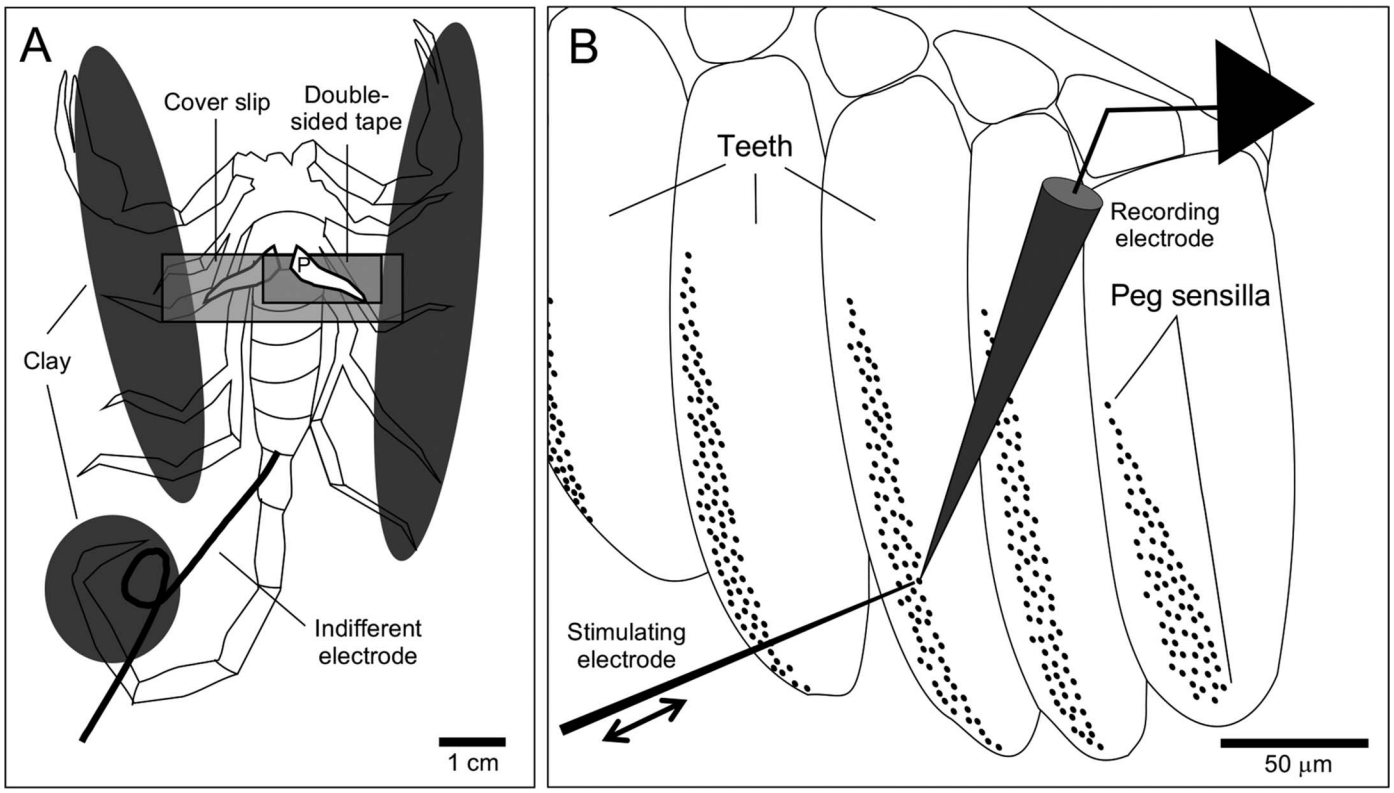

Figure 1.—Scorpion recording preparation. A. The scorpion is secured with clay to a microscope slide ventral side up, and the left pecten (P) is lifted and placed on double-sided tape atop a cover slip. An indifferent electrode is inserted between body segments. B. Fields of peg sensilla occupy the ground-facing surfaces of pectinal teeth. The recording electrode is placed in the base of a single peg sensillum and stimulating electrode is advanced to physically push the recorded peg.

than males and are therefore good models for assessing navigation in central place foragers (Polis et al. 1985). We used eleven of these animals to refine our recording techniques, learn how best to position the pectines and equipment, and determine the best way to deflect the pegs to elicit a mechanoreceptor response. The results presented in this article represent the three recordings from three different animals with the highest signal-to-noise ratio and clearest mechanoreceptor response.

Preparation for electrophysiology.—To prepare for electrophysiology, a scorpion was removed from its jar and placed into a small glass dish in the freezer (at −11°C for 1–2 minutes). Once the scorpion was temporarily sedated, it was placed ventral side up on a glass microscope slide to expose the pectines (Fig. 1A). A round piece of clay was placed to secure the tail, and two long cylindrical pieces of clay were placed parallel to the body to secure the legs and pedipalps on either side of the body. A cover slip (CS) was cut in half using a diamond tip pencil and sanded to dull the cut edge. A piece of double-sided tape was placed on the CS, and the slip was placed on top of the pectines. Small pieces of clay were placed on the edges of the CS to further secure it in place. We then used fine tipped forceps to pull the left pecten from below the CS and place it atop the tape. We carefully pressed the pecten and the teeth into the tape using a fine tipped brush. Finally, we made an indifferent electrode by using a razor blade to cut one end of a 5 cm length of silver wire to a sharp point that we inserted between body segments of the tail until a small amount of hemolymph was seen when the wire was slightly withdrawn. The free end of the wire was secured with clay and the prepared scorpion slide was then placed on a micromanipulator and positioned under the microscope to begin recording.

Mechanoreceptor recording from individual peg sensilla.—We used the microscope (Olympus BX50WI light microscope with long working distance objectives and epi-illumination) under 250x and 650x magnification to locate a patch of pegs. The stimulating electrode (SE) consisted of a 3 cm long tungsten wire sharpened to a relatively blunt tip (~3 μm) that protruded from a syringe needle. The syringe needle was then attached to a pneumatic-driven manipulator (Olympus model ONO-111) that was further held on a Leitz micromanipulator with fine joystick control. We used the Leitz manipulator to move the SE into focus and lower it to the same field of view as the pegs. The tungsten recording electrode (RE) was electrolytically carved to a tip diameter of ~1 μm, held in a syringe needle, and attached to a second Leitz micromanipulator (also with joystick control). The RE tip was carefully maneuvered to the target peg and inserted through the flexible cuticle at the peg base until extracellular neural activity was detected. The RE was inserted only until an initial reading was established to ensure that the peg remained exposed for mechanical manipulation. The recordings were amplified 10,000x using an AC differential amplifier (DAM 80, World Precision Instruments), bandpass filtered between 300 Hz and 1 kHz, and sampled at 15 kHz by an analog to digital board (1401-micro-3, Cambridge Electronics Design, Cambridge, UK). Once the RE was placed, the SE was further positioned to be directed toward the recorded peg and the pneumatic drive was then used to advance the SE tip to lightly push the recorded peg (Figure 1B). The entire preparation (animal, microscope, manipulators) rested atop a heavy metal table (Technical Manufactory Corporation, Peabody, MA) that floated on nitrogen to eliminate room vibrations and was

surrounded by a grounded Faraday cage to reduce extraneous electrical noise. The raw records were captured, stored, and initially processed using *Spike 2* software (Cambridge Electronics Design).

Testing the graded response based on duration of stimulation.—The graded response was first tested by applying two different durations of mechanical stimulation. The first was a shorter-duration stimulation in which the SE was advanced approximately 6 μm to touch and push the peg and was immediately pulled back from the peg (<0.5 s) in which the RE was inserted. The other stimulation was a longer-duration stimulation where the SE was also advanced approximately 6 μm to push the peg in which the RE was inserted and it was left for 0.5–1.0 s before pulling back. At least ten touches of each stimulation type ("short" or "long") were initiated, with a 5 s recovery period between each stimulation. While the stimulations were made by hand, we monitored the real time *Spike 2* display to control the stimulus durations as much as possible.

Testing the graded response based on distance of stimulation.—The graded response was further tested using two different distances of mechanical stimulations. The first was a smaller deflection in which the SE was advanced between 6–8 μm to push the peg in which the RE was inserted. The SE was immediately pulled back to the starting position once the total distance was traveled. The second stimulation type was a larger deflection in which the SE was advanced 10–12 μm to push the peg in which the RE was inserted; again, the SE was immediately pulled back to the starting position once the total distance was traveled. To calibrate the distance of travel of the electrode tip, we used the microscope to monitor the tip travel relative to a micro ruler. We then made marks on the dial of the micromanipulator to indicate the two different distances and used these marks as our guide during our trials. We reduced the interstimulus interval to about 2.5 s in these trials and alternated the two stimulation types throughout the recording to avoid potential adaptation to repetitions of a given stimulus type.

Record analysis.—Each of the electrophysiology recordings was analyzed through a combination of Spike2 and a specially written MATLAB script. The MATLAB script was crucial for refining the spike categorizations and for generating response plots, autocorrelograms, and graphs of instantaneous spiking frequency.

RESULTS

Identifying the mechanoreceptor waveform.—Our baseline recordings from peg sensilla showed spontaneous low spiking frequency of previously identified A and B chemosensory waveforms (Gaffin & Shakir 2021). Deflection of the peg shaft with the SE induced activity of a distinct rapid firing, quickly adapting waveform (termed "M") that had a larger amplitude negative phase (~0.25 mV more negative) compared to the A and B waveforms. Fig. 2 shows a high-fidelity record with 26 mechanical stimulations (each ~10 μm distance and ~1 s duration) where the spike forms resolved well. The M spike waveform was also distinguishable from the A type spikes by the gentle slope of its recovery phase at the end of its waveform (see Fig. 2A, superimposed spikes). An auto-correlogram of the M spikes (where each identified spike is time referenced against all other spikes of the same type) shows both a clear refractory period (note the lack of spikes around time 0 in the inset below the superimposed M spikes of Fig. 2A) and that the M spikes are capable of very high frequency activity. This activity level can be deduced from the auto-correlogram by noting that some M spikes fire within 0.005 s (5 ms) of the referenced spikes; a 5 ms inter-spike interval translates to 200 Hz (=1/0.005 s). The B cells also resolved well and had the characteristic "glitch" in the negative-going phase of their waveforms (Gaffin & Shakir 2021). The B cell auto-correlogram also produced a clear refractory period, but the peak frequency of the B cells was only about 10 Hz (=1/0.1 s). The auto-correlogram of the A cells did not yield a clear refractory period around the origin. This result was not surprising since two A type cells (A_1 and A_2) often superimpose (Gaffin & Shakir 2021) and are difficult to isolate, as was the case in the record shown in Fig. 2. The peak activity of the A cells in the record was also in the range of 10 Hz.

To examine the dynamics of the mechanosensory response, we clipped, aligned, and superimposed the 26 stimulations coded by spike type (Fig. 2B, upper trace) and plotted instantaneous firing frequencies of the three spike types along with the average spiking frequencies for the three cell types during these stimulations (Fig. 2B, lower plot). Fig. 2C shows the average spiking frequencies (± SEM) of the three spike types binned by 0.05 s. The record shows a phasic increase in the spiking frequency of the M waveform that quickly returns to ~0 Hz within a second following stimulation; also note the absence of stimulus-related responses by neurons A and B.

Graded responses.—The first test of a putative graded mechanosensory response of the peg sensilla compared short-duration (Fig. 3A) to long-duration (Fig. 3B) touches. This test once again produced high-frequency firing of mechanosensory waves that corresponded to the initiation of the stimulation for both the touch types. The M and A waveforms did not resolve as well as in the example shown in Fig. 2, although autocorrelations of the M spikes (not shown) again produced a clear refractory period. To avoid mislabeling of cell types, we assessed composite spiking activity without regards to spike classification. While the initial spiking frequencies were similar between the two types of stimulations, the long touches sustained higher spiking activity for several tenths of a second as compared to the short touches (Fig. 3C). Both stimulation types showed a pattern of rapid adaptation. Further, both stimulation types showed small subsequent increases in spiking activity: short touches at 0.40 s and long touches at 0.65 s post-stimulus initiation. These secondary increases likely reflect mechanosensory activity induced by the removal of the SE, allowing the return of the peg to its initial upright state.

The second graded response test compared a small deflection (6–8 μm) to a large deflection (10–12 μm). This test produced the same high frequency, quickly adapting response patterns seen in the previous stimulations. In the example shown in Fig. 4, 29 small and 29 large deflections were interspersed across the record and spaced an average of 2.5 s apart. Again, the spikes were pooled in these records without regard to classification. The large deflections generated greater initial spiking frequencies than the small deflections, and while both stimulation types showed rapid adaptation, the large deflection spiking frequencies remained higher than the small deflection frequencies across the entire response (Fig. 4D). Once again, a slight secondary recovery occurred in the large deflection stimulations (around 0.8 s) that likely corresponded with the retraction of the SE. There was no discernable decline in the initial response frequencies across the 58 stimulations, which indicates that the mechanosensory cell fully recovers within the 2.5 s inter-stimulus interval.

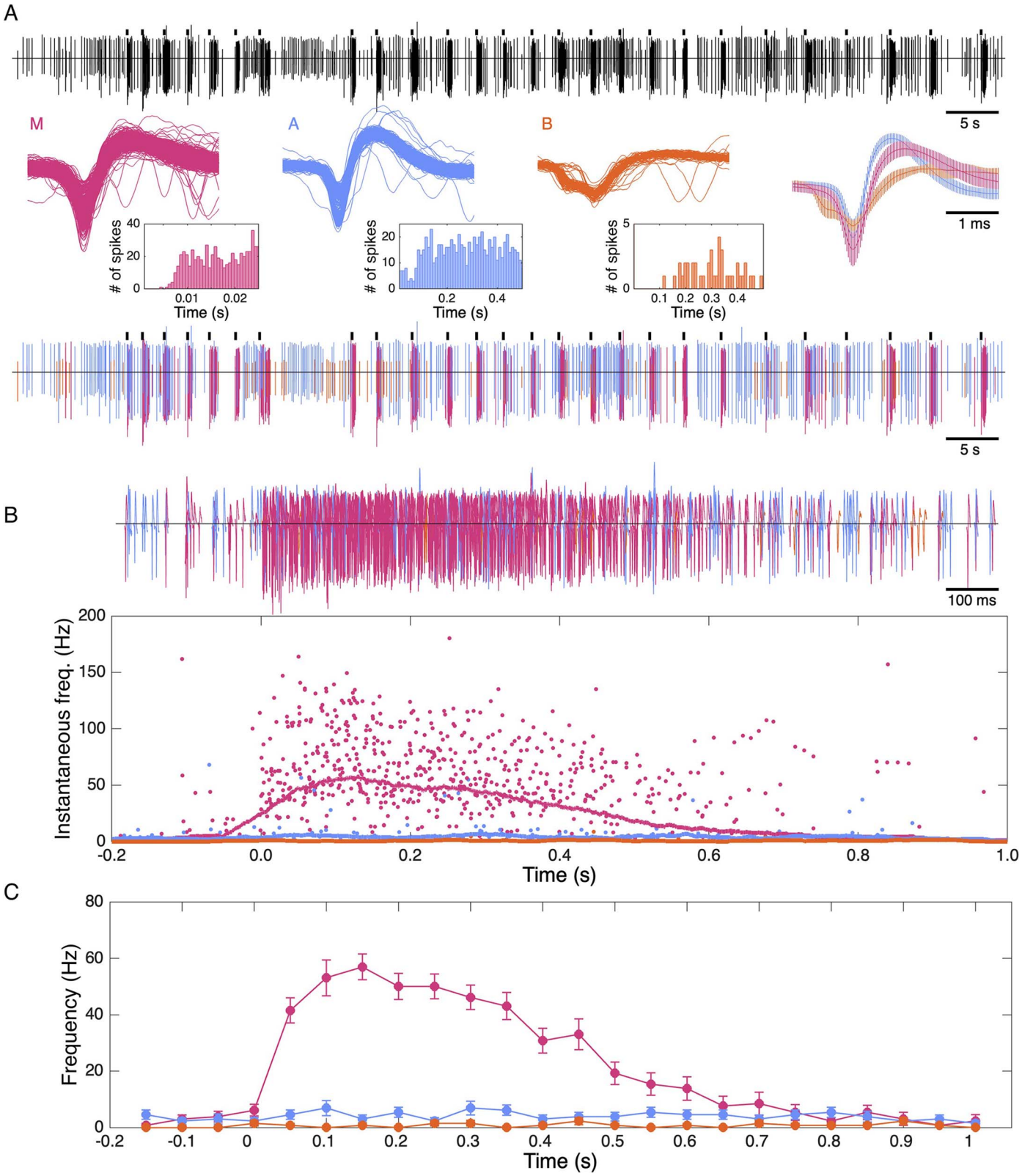

Figure 2.—Sample mechanosensory response. A. Upper panel: Raw electrophysiological recording (~100 s) containing 26 stimulation points indicated with tick marks at top. Middle panel: Overlays of the M, A, and B waveforms along with superimposed average waveforms (± SD) at right. Insets are autocorrelograms for each of the spike types. Lower panel: The same electrophysiological trace as in the upper panel has been color-coded based on spike classification. B. Upper panel: The 26 stimulations have been expanded (0.2 s pre-stimulus, 1.0 s post-stimulus) and superimposed. Lower panel: Instantaneous spiking frequencies for all 26 stimulations are plotted for the three spike types (lines indicate mean spiking frequency for each spike type). C. The mean spiking frequencies (± SEM) are plotted by 0.05 s bins for the three spike types relative to the initiation of mechanical stimulation (time zero).

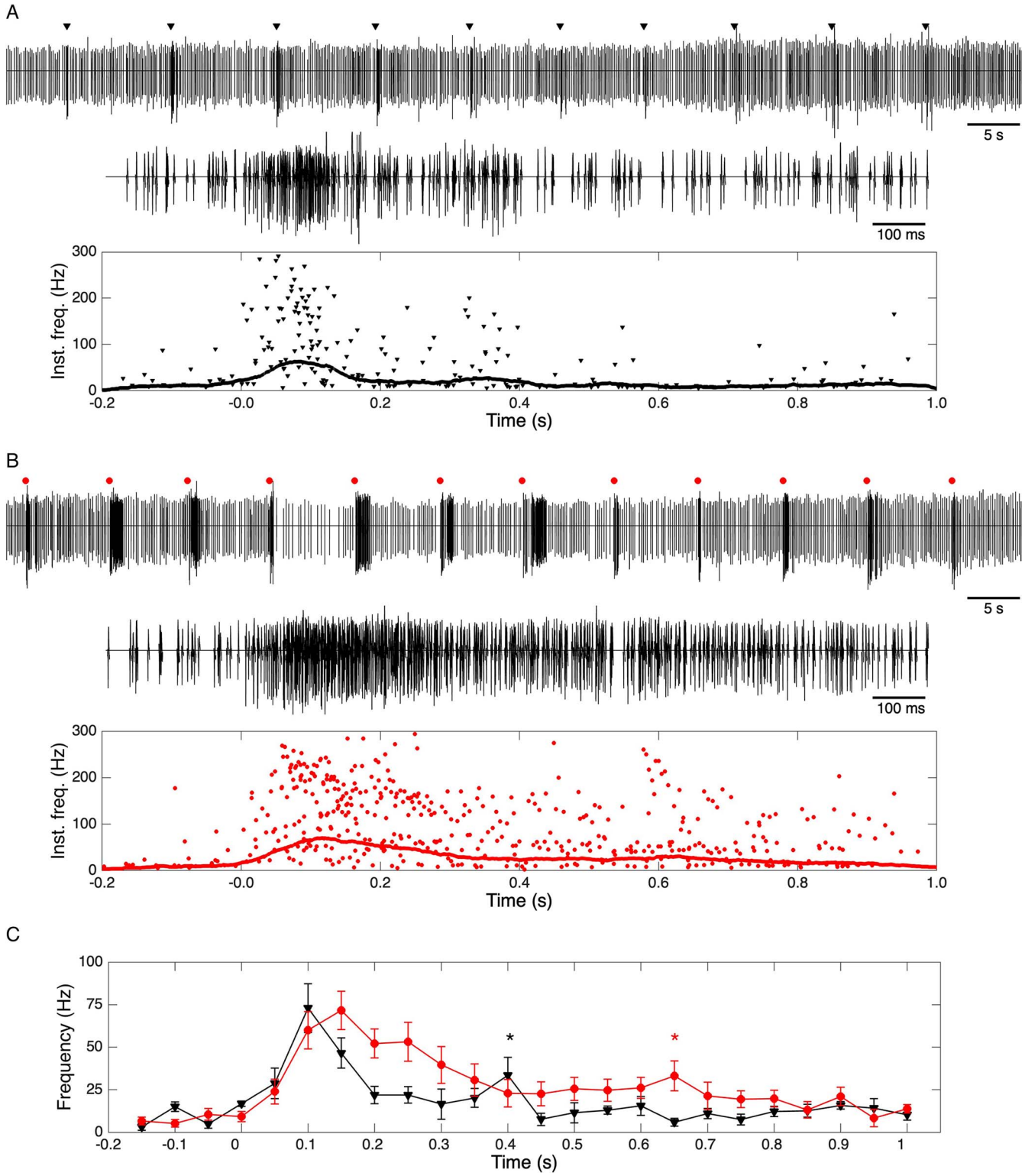

Figure 3.—Comparison of the short-duration versus the long-duration stimulations. A. Upper panel: An electrophysiological recording containing 10 "short" stimulation points (black triangles). Middle panel: The 10 stimulations are expanded (0.2 s pre-stimulus, 1.0 s post-stimulus) and superimposed. Lower panel: The instantaneous spiking frequencies for all spikes combined are plotted relative to the mechanical stimulation (black line indicates mean spiking frequency for all spikes in the record). B. Upper panel: An electrophysiology recording containing 12 "long" stimulation points (red circles). Middle panel: The 12 stimulations are expanded (0.2 s pre-stimulus, 1.0 s post-stimulus) and superimposed. Lower panel: The instantaneous spiking frequencies for all spikes combined are plotted relative to the mechanical stimulation (red line indicates mean spiking frequency for all spikes in the record). C. The average spiking frequencies (± SEM) are plotted by 0.05s bins for the short-duration (black triangles) and long-duration (red circles) stimulations. Small, secondary post-stimulus peaks are noted by asterisks (red = short-duration at 0.40 s; black = long-duration at 0.65 s).

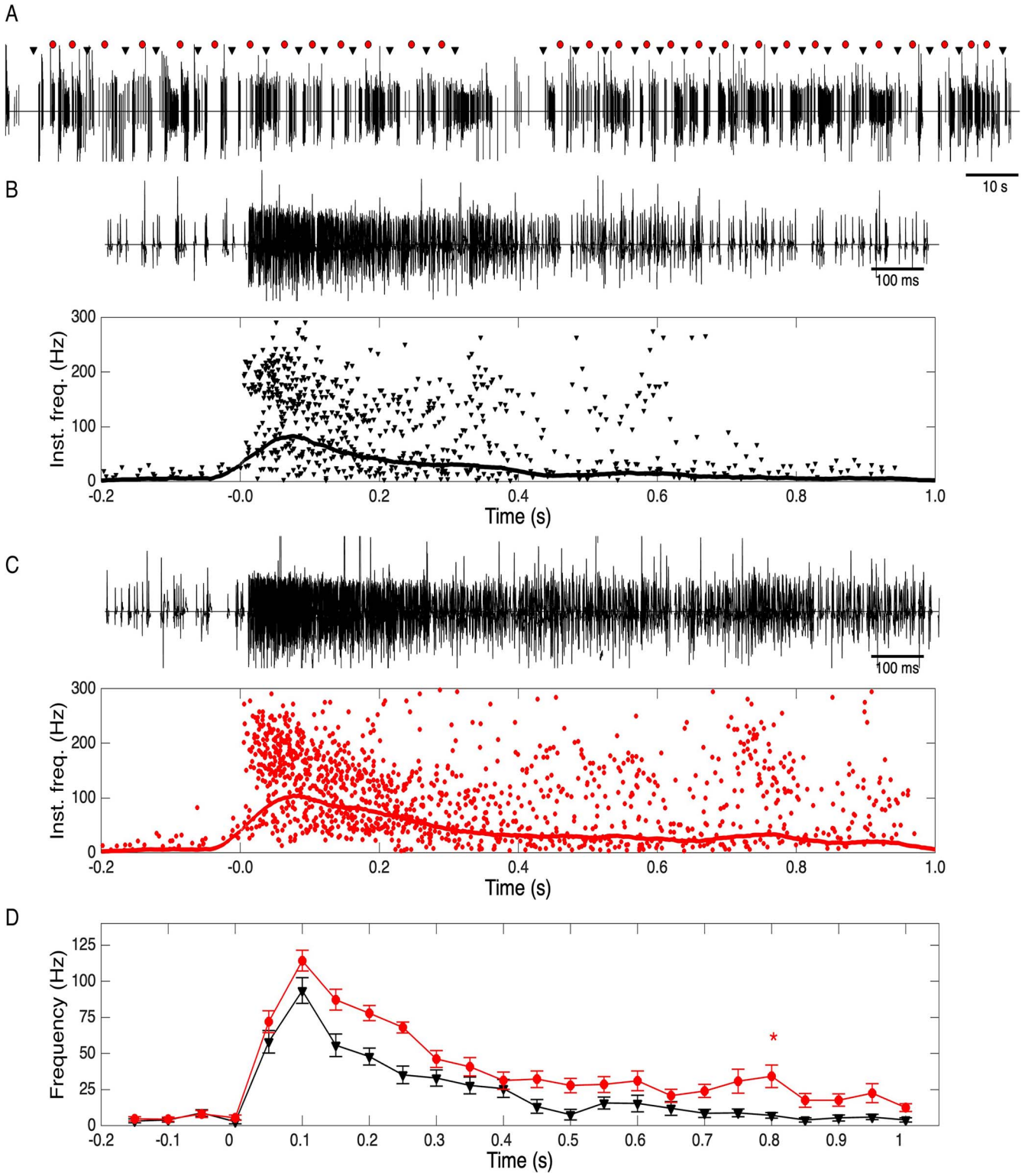

Figure 4.—Comparison of the small versus large deflections. A. An electrophysiological recording containing 29 small deflections (black triangles) interspersed with 29 large deflections (red circles). B. Upper panel: The small deflection responses are expanded (0.2 s pre-stimulus, 1.0 s post-stimulus) and superimposed. Lower panel: The instantaneous spiking frequencies for all spikes combined are plotted relative to the time of deflection (black line indicates mean spiking frequency for all spikes in the record). C. Upper panel: The large deflection responses are expanded (0.2 s pre-stimulus, 1.0 s post-stimulus) and superimposed. Lower panel: The instantaneous spiking frequencies for all spikes combined are plotted relative to the time of deflection (red line indicates mean spiking frequency for all spikes in the record). D. The average spiking frequencies (± SEM) are plotted by 0.05s bins for the small distance (black triangles) and long distance (red circles) deflections. A small, secondary post-stimulus peak is noted by red asterisk at 0.80 s.

DISCUSSION

We identified a mechanosensory waveform that consistently fired in response to peg deflection and that was distinguishable from previously identified chemosensory waveforms. Furthermore, we found that only one type of mechanosensory waveform was induced in each of our many recordings and that the pattern of the mechanosensory response was similar in all our records: a phasic response pattern of high-frequency activity of mechanosensory waveforms that quickly adapted and quickly recovered. Also, while our preparation restricted us to deflecting the pegs in only one direction, the secondary increase in spiking activity seen in some of our records after the stimulus electrode was withdrawn suggests that the mechanosensory cell might respond to the release of deflection. It therefore seems possible that a stimulus coming from the opposite direction could also generate high frequency responses. However, these response dynamics may be related to the asymmetry of the mechanosensory cell insertion point at the base of each peg sensillum (Foelix & Müller-Vorholt 1983). Unfortunately, the limits of the light microscopy used in our preparation did not allow us to resolve peg deflection direction relative to mechanosensory cell insertion point.

We also found through a series of specific stimulations that the mechanosensory responses appear graded, as opposed to "all-or-none" (or binary). There were clear differences between the response profiles of short vs long stimulations and small vs large deflections. In these simple tests, we can therefore identify at least three response states, perhaps seen best in the small vs large deflection stimulations (Fig. 4). For example, the large deflection generated average initial spiking frequencies of about 120 Hz while the small deflection frequencies were about 90 Hz. Of course, a third state exists in the absence of any deflection (0 Hz). While we recognize that graded responses are smoothly varying, for the purposes of this discussion we consider different states to be identifiable based on statistically discernable differences. Many additional response states are possible but detecting them would require tests with more refined and subtle stimulation capabilities.

Our data are clearly pointing to graded responses from the mechanosensory cells, and this insight adds to our model of how scorpions might interpret the textures of their environment. The pegs can be considered as a matrix in which specific deflection patterns and intensities are being interpreted by the scorpion central nervous system (CNS) (Gaffin & Brayfield 2017; Musaelian & Gaffin 2020). The importance of the matrix can be explained with a simple 4-point example. If a 2x2 grid only contains black and white squares (as in a binary, "all or none" scenario), there are two options (or states) with four square locations. The number of possible patterns can be determined by raising the number of states to the number of squares. In this case, 2^4 produces 16 possible combinations. If a 2x2 grid contains a shade of gray in addition to black and white, the number of possible states increases to three, and the number of possible patterns increases greatly to 3^4 or 81 combinations.

By applying the graded response to scorpions' pectines, the possible number of detectable patterns grows precipitously. Each tooth extending from the scorpion pecten of female *P. utahensis* scorpions contains at least 100 peg sensilla (Gaffin & Walvoord 2004). In matrix language, using the minimum of three states of the mechanosensory response suggested in this paper, the number of possible detectable patterns for a single tooth is 3^{100} (or $5.15*10^{47}$). A female scorpion's pecten contains approximately 21 teeth, and all scorpions have two pectines. Therefore, the calculation for the combined 42 teeth would be 3^{4200} (3^2*21*100)!

Another factor to consider is the size of a sand granule as compared to the size of a single peg sensillum. *Paruroctonus utahensis* is a desert sand scorpion, and the substrate on which they navigate consists mainly of small sand granules. The pegs are spaced approximately 7 μm apart, while sand particles from the animals' natural habitat are on the order of 150 μm diameter (Brownell 2001; Gaffin & Walvoord 2004). As such, in terms of scale, the pectinal teeth are more in line with the particulate nature of the sand substrate than individual peg sensilla; a sand grain can span about 2–3 teeth or hundreds of pegs (Gaffin & Walvoord 2004). We therefore suspect that the tooth might be the basic unit of information at the level of the CNS. Applying the matrix example here, each tooth has 300 possible states (since each peg has at least three states and there are ~100 pegs per tooth). For the combined 42 teeth, the total textural resolvability for a scorpion under this model would therefore be $300^{42} = 1.09*10^{104}$. Simply put, scorpion pectines have the potential to resolve an enormous number of textural patterns, regardless of the unit of information. Furthermore, it is likely that there are more than just three states of the mechanosensory response, which would further increase textural resolvability.

Additional research regarding the mechanosensory abilities of the peg sensilla should add additional degrees of stimulus deflection as well as deflections that come from various directions to see if a directional bias exits in the mechanosensory response. It would also be helpful to reduce variability by using an automated programable device instead of a manual manipulator to control the SE. In addition, recording from the scorpion suboesophageal ganglion while deflecting the peg would help reveal how the information is being interpreted by the CNS. Finally, the textural discrimination models need to be tested through behavioral studies. For example, navigational tests might be run with animals on smooth glass substrates versus glass substrates with added textural incongruities. We predict that homing accuracy would increase with textural complexity.

ACKNOWLEDGMENTS

We thank Alexis Merchant for feedback and assistance in the lab, Mariëlle Hoefnagels for constructive criticism and editing assistance, George Martin for engineering assistance, and Sandra Doan and Gail Goodson for help caring for the animals. We also thank the University of Oklahoma Honors College and Biology Department for facilities support, and the University of Oklahoma Foundation and the Undergraduate Research Opportunities Program for funding support. We thank foreman Ronnie Miller with the Sealy-Smith Foundation in Monahans, TX for allowing us to collect animals on their land and Arturo Taveras for help with our field logistics. Finally, we thank the reviewers for their thoughtful comments and suggestions that have improved the quality of the manuscript.

LITERATURE CITED

Brownell PH. 1998. Glomerular cytoarchitectures in chemosensory systems of arachnids. *Annals of the New York Academy of Sciences* 855:502–507.

Brownell P. 2001. Sensory ecology and orientational behaviors. Pp. 159–183. *In* Scorpion Biology and Research. (P. Brownell & G. Polis, eds.). Oxford University Press

Drozd D, Wolf H, Stemme T. 2020. Structure of the pecten neuropil pathway and its innervation by bimodal peg afferents in two scorpion species. *PLOS ONE* 15:e0243753.

Drozd D, Wolf H, Stemme T. 2022. Mechanosensory pathways of scorpion pecten hair sensillae—Adjustment of body height and pecten position. *Journal of Comparative Neurology* n/a:1–20. https://doi.org/10.1002/cne.25384

Foelix R, Müller-Vorholt G. 1983. The fine structure of scorpion sensory organs. ii.pecten sensilla. *Bulletin British Arachnological Society* 6: 68–74.

Gaffin D. 2001. Electrophysiological properties of sensory neurons in peg sensilla of *Centruroides vittatus* (say, 1821) (Scorpiones: Buthidae). Pp. 325–330. *In* Scorpions 2001. In Memoriam Gary A. Polis. Burnham Beeches, Bucks: British Arachnological Society.

Gaffin DD, Brayfield BP. 2017. Exploring the chemo-textural familiarity hypothesis for scorpion navigation. *Journal of Arachnology* 45:265–270.

Gaffin DD, Brownell PH. 1992. Evidence of chemical signaling in the sand scorpion, *Paruroctonus* mesaensis (Scorpionida: Vaejovidae). *Ethology* 91:59–69.

Gaffin DD, Brownell PH. 1997. Response properties of chemosensory peg sensilla on the pectines of scorpions. *Journal of Comparative Physiology A* 181:291–300.

Gaffin DD, Brownell PH. 2001. Chemosensory behavior and physiology. Pp. 184–203. *In* Scorpion Biology and Research. (P. Brownell & G. Polis, eds.). Oxford University Press.

Gaffin DD, Curry CM. 2020. Arachnid navigation – a review of classic and emerging models. *Journal of Arachnology* 48:1–25.

Gaffin DD, Shakir SF. 2021. Synaptic interactions in scorpion peg sensilla appear to maintain chemosensory neurons within dynamic firing range. *Insects* 12:904. https://doi.org/10.3390/insects12100904

Gaffin DD, Walvoord ME. 2004. Scorpion peg sensilla: are they the same or are they different? *Euscorpius* 17:1–9.

Gaffin DD, Muñoz MG, Hoefnagels MH. 2022. Evidence of learning walks related to scorpion home burrow navigation. *Journal of Experimental Biology* 225:jeb243947. https://doi.org/10.1242/jeb.243947

Hughes KL, Gaffin DD. 2019. Investigating sensory processing in the pectines of the striped bark scorpion, *Centruroides vittatus*. *Invertebrate Neuroscience* 19:9. https://doi.org/10.1007/s10158-019-0228-8

Ivanov V, Balashov Y. 1979. The structural and functional organization of the pectine in a scorpion *Buthus eupeus* Koch (Scorpiones, Buthidae) studied by electron microscopy. *Fauna i ekologiya paukoobraznykh. Trudy Zoologicheskogo Instituta (Leningrad)* 85:73–81.

Knowlton ED, Gaffin DD. 2009. A new approach to examining scorpion peg sensilla: the mineral oil flood technique. *Journal of Arachnology* 37:379–382.

Knowlton ED, Gaffin DD. 2010. A new tip-recording method to test scorpion pecten chemoresponses to water-soluble stimulants. *Journal of Neuroscience Methods* 193:264–270. https://doi.org/10.1016/j.jneumeth.2010.09.002

Knowlton ED, Gaffin DD. 2011a. Electrophysiology of scorpion peg sensilla. *Journal of Visualized Experiments* e2642.

Knowlton ED, Gaffin DD. 2011b. Functionally redundant peg sensilla on the scorpion pecten. *Journal of Comparative Physiology A* 197:895. https://doi.org/10.1007/s00359-011-0650-9

Krapf D. 1986. Contact chemoreception of prey in hunting scorpions (Arachnida: Scorpiones). *Zoologischer Anzeiger* 217:119–129.

Melville JM, Tallarovic SK, Brownell PH. 2003. Evidence of mate trailing in the giant hairy desert scorpion, *Hadrurus arizonensis* (Scorpionida, Iuridae). *Journal of Insect Behavior* 16:97–115.

Musaelian A, Gaffin DD. 2020. High-throughput simulations indicate feasibility of navigation by familiarity with a local sensor such as scorpion pectines. *bioRxiv* 2020.06.17.156612.

Ortega-Escobar J, Hebets EA, Bingman VP, Wiegmann DD, Gaffin DD. 2023. Comparative biology of spatial navigation in three arachnid orders (Amblypygi, Araneae, and Scorpiones). Journal of Comparative Physiology A, https://doi.org/10.1007/s00359-023-01612-2

Polis GA, Farley RD. 1979. Behavior and ecology of mating in the cannibalistic scorpion, *Paruroctonus mesaensis* Stahnke (Scorpionida: Vaejovidae). *Journal of Arachnology* 7:33–46.

Polis GA, McReynolds CN, Ford RG. 1985. Home range geometry of the desert scorpion *Paruroctonus mesaensis*. *Oecologia* 67:273–277.

Prévost ED, Stemme T. 2020. Non-visual homing and the current status of navigation in scorpions. *Animal Cognition* 23:1215–1234.

Taylor MS, Cosper CR, Gaffin DD. 2012. Behavioral evidence of pheromonal signaling in desert grassland scorpions *Paruroctonus utahensis*. *Journal of Arachnology* 40:240–244.

Wolf H. 2008. The pectine organs of the scorpion, *Vaejovis spinigerus*: structure and (glomerular) central projections. *Arthropod Structure & Development* 37:67–80.

Wolf H. 2017. Scorpions pectines – Idiosyncratic chemo- and mechanosensory organs. *Arthropod Structure & Development* 46:753–764.

Wolf H, Harzsch S. 2012. Serotonin-immunoreactive neurons in scorpion pectine neuropils: similarities to insect and crustacean primary olfactory centres? *Zoology* 115:151–159.

Manuscript received 19 August 2022, revised 7 November 2022, accepted 8 November 2022.